Image-Domain Material Decomposition Using Data-Driven Sparsity Models for Dual-Energy CT

Zhipeng Li[1], Saiprasad Ravishankar[2], Yong Long[1], Jeffrey A. Fessler[2]

[1]University of Michigan - Shanghai Jiao Tong University Joint Institute,
Shanghai Jiao Tong University, Shanghai, China
[2]Department of Electrical Engineering and Computer Science,
University of Michigan, MI, USA

April 5, 2018

Outline

- Dual-Energy CT (DECT)
  - Enables characterizing concentration of constituent materials in scanned objects, known as material decomposition[1]

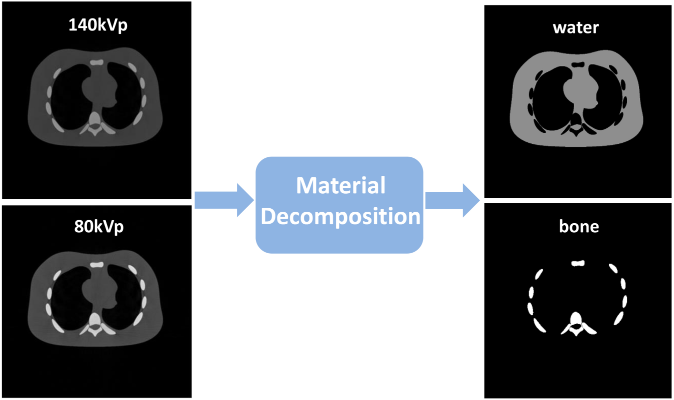

[1] [Mendonca et al., IEEE T-MI, 2014]

Image measurements (attenuation maps at high and low energy) are directly available on commercial DECT scanners

- Conventional image-domain decomposition
  - Direct matrix inversion decomposition[2]
  - Susceptible to artifacts and noise.
- Regularized (model-based) decomposition
  - Statistical measurement model + Object prior model
  - Improves image quality and decomposition accuracy

[2] [Niu et al., MP, 2014]

Regularization Approches for DECT

- Non-adaptive regularization
  - Material-wise Edge-Preserving (EP) [3]
    - Suppress noise while retaining boundary sharpness
    - Use simple prior models

[3] [Xue et al., MP, 2017]
[4] [Li et al., ISBI, 2012]
[5] [Chen & Li, F3D 2017]

Regularization Approches for DECT

- Non-adaptive regularization
  - Material-wise Edge-Preserving (EP) [3]
    - Suppress noise while retaining boundary sharpness
    - Use simple prior models
- Learning-based regularization
  - Dictionary Learning
    - have shown promising results for DECT[4]
    - highly non-convex and NP-Hard sparse coding
    - Computation: $O(m^3N)$
      m is patch size, N is the number of patches
  - Deep learning for spectral CT[5] $O(?)$
  - Sparsifying Transform (ST) learning
    - DECT-ST: proposed approach
    - Computation: $O(m^2N)$

[3] [Xue et al., MP, 2017]
[4] [Li et al., ISBI, 2012]
[5] [Chen & Li, F3D 2017]

Material-Wise Sparsifying Transform (ST)

- Sparsifying Transform Learning[6]:
  - A generalized analysis operator learning approach
  - Closed-form solutions for simple thresholding-based sparse coding

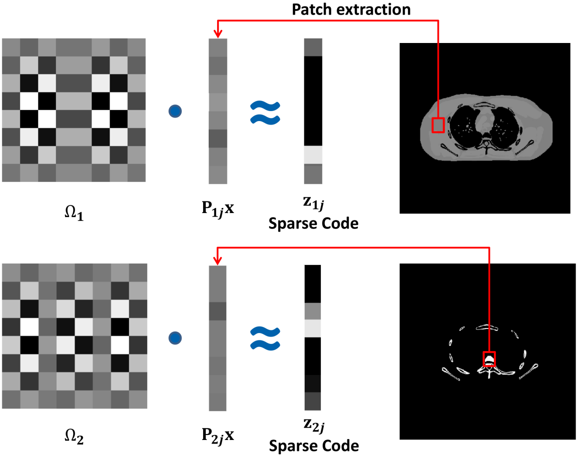

6 [Ravishankar & Bresler, IEEE T-SP, 2015]

Outline

Learn two sparsifying transforms independently, for material $l = 1, 2$:

$$\arg\min_{\boldsymbol{\Omega}_l} \min_{\mathbf{Z}_l} \overbrace{\|\boldsymbol{\Omega}_l \mathbf{Y}_l - \mathbf{Z}_l\|_F^2}^{\text{Sparsification error}} + \overbrace{\lambda \left(\|\boldsymbol{\Omega}_l\|_F^2 - \log|\det \boldsymbol{\Omega}_l|\right)}^{\text{Transform regularizer}} + \overbrace{\sum_{i=1}^{N'} \eta^2 \|\mathbf{Z}_{li}\|_0}^{\text{Non-sparse penalty}}$$

- $\boldsymbol{\Omega}_l$: $m \times m$ square transform to be learned for lth material type
- $\mathbf{Y}_l$: $m \times N'$ matrix of training patches from lth material images
- $\mathbf{Z}_l$: $m \times N'$ matrix of sparse codes of $\mathbf{Y}_l$ (discard after training)
- $\|\boldsymbol{\Omega}_l\|_F^2 - \log|\det \boldsymbol{\Omega}_l|$: prevents trivial solutions, controls transform condition number[7]
- Training ST uses an efficient alternating algorithm

[7] [Ravishankar & Bresler, IEEE T-SP, 2015]

Optimization problem:

$$\arg\min_{\mathbf{x}\in\mathbb{R}^{2N_p}} \min_{\{\mathbf{z}_{lj}\}} \frac{1}{2}\|\mathbf{y}-\mathbf{A}\mathbf{x}\|_{\mathbf{W}}^2 + \sum_{l=1}^{2}\sum_{j=1}^{N} \beta_l \left\{ \|\boldsymbol{\Omega}_l \mathbf{P}_{lj}\mathbf{x} - \mathbf{z}_{lj}\|_2^2 + \gamma_l^2 \|\mathbf{z}_{lj}\|_0 \right\}$$

- $\mathbf{y} = (\mathbf{y}_H^T, \mathbf{y}_L^T)^T \in \mathbb{R}^{2N_p}$: attenuation maps at high and low energy
- $\mathbf{x} = (\mathbf{x}_1^T, \mathbf{x}_2^T)^T \in \mathbb{R}^{2N_p}$: unknown material density images
- $\mathbf{A} = \mathbf{A}_0 \otimes \mathbf{I}_{N_p}$: matrix of (calibrated) mass attenuation coefficients:

$$\mathbf{A}_0 = \begin{pmatrix} \varphi_{1H} & \varphi_{2H} \\ \varphi_{1L} & \varphi_{2L} \end{pmatrix}.$$

- $\mathbf{W} = \mathbf{W}_j \otimes \mathbf{I}_{N_p}$: weight matrix with $\mathbf{W}_j = \mathrm{diag}(\sigma_H^2, \sigma_L^2)^{-1}$
- $\mathbf{P}_j \in \mathbb{R}^{m\times N_p}$: extracts the jth patch of $\mathbf{x}_l$ as a vector $\mathbf{P}_j\mathbf{x}$
- $\mathbf{z}_{lj} \in \mathbb{R}^m$: sparse codes of $\mathbf{P}_{lj}\mathbf{x}$
- N: number of image patches

Outline

Sparse Coding Step

Overall optimization problem:

$$\arg\min_{\mathbf{x}\in\mathbb{R}^{2N_p}} \min_{\{\mathbf{z}_{lj}\}} \frac{1}{2}\|\mathbf{y}-\mathbf{A}\mathbf{x}\|_{\mathbf{W}}^2 + \sum_{l=1}^{2}\sum_{j=1}^{N}\beta_l\left\{\|\boldsymbol{\Omega}_l\mathbf{P}_{lj}\mathbf{x}-\mathbf{z}_{lj}\|_2^2+\gamma_l^2\|\mathbf{z}_{lj}\|_0\right\}$$

- Sparse code update:

$$\begin{aligned}\{\hat{\mathbf{z}}_{lj}\} &= \arg\min_{\{\mathbf{z}_{lj}\}} \sum_{l=1}^{2}\sum_{j=1}^{N}\beta_l\left\{\|\boldsymbol{\Omega}_l\mathbf{P}_{lj}\mathbf{x}-\mathbf{z}_{lj}\|_2^2+\gamma_l^2\|\mathbf{z}_{lj}\|_0\right\} \\ \hat{\mathbf{z}}_{lj} &= H_{\gamma_l}(\boldsymbol{\Omega}_l\mathbf{P}_{lj}\mathbf{x})\end{aligned} \quad (1)$$

- Hard-thresholding operator $H_\gamma(b)$: returns 0 if $|b|<\gamma$

Image Update Step - Quadratic Majorizer

$$\min_{\mathbf{x}\in\mathbb{R}^{2N_p}} \frac{1}{2}\|\mathbf{y}-\mathbf{A}\mathbf{x}\|_{\mathbf{W}}^2 + \overbrace{\sum_{l=1}^{2}\sum_{j=1}^{N}\beta_l \|\boldsymbol{\Omega}_l \mathbf{P}_{lj}\mathbf{x} - \mathbf{z}_{lj}\|_2^2}^{\mathsf{R}_2(\mathbf{x})} \tag{2}$$

- Quadratic majorizer $\psi_{\mathbf{M}}(\mathbf{x}, \mathbf{u}^{(i)})$ at the ith iteration:

$$\psi_{\mathbf{M}}(\mathbf{x}; \mathbf{u}^{(i)}) = \frac{1}{2}\|\mathbf{x} - \boldsymbol{\xi}^{(i)}\|_{\mathbf{M}}^2 \tag{3}$$

where $\boldsymbol{\xi}^{(i)} = \mathbf{u}^{(i)} - \mathbf{M}^{-1}\nabla\mathsf{R}_2(\mathbf{u}^{(i)})$.

- Image update:

$$\mathbf{x}^{(i+1)} = \arg\min_{\mathbf{x}} \frac{1}{2}\|\mathbf{y}-\mathbf{A}\mathbf{x}\|_{\mathbf{W}}^2 + \psi_{\mathbf{M}}(\mathbf{x}; \mathbf{u}^{(i)}), \tag{4}$$

Image Update Step - Majorizing Matrix

- Design of the diagonal majorizing matrix $\mathbf{M}$:

$$\mathbf{M} \succeq \nabla^2 \mathsf{R}_2(\mathbf{x}) = 2 \sum_{l=1}^{2} \beta_l \sum_{j=1}^{N} \mathbf{P}_{lj}' \boldsymbol{\Omega}_l{}' \boldsymbol{\Omega}_l \mathbf{P}_{lj}. \quad (5)$$

- With patch stride of 1 pixel, the entries of the diagonal matrix $\sum_{j=1}^{N} \mathbf{P}_{lj}' \mathbf{P}_{lj}$ corresponding to the lth material are equal to $m\mathbf{I}_{N_p}$
- Diagonal majorizer $\mathbf{M}$:

$$\mathbf{M} = \begin{pmatrix} 2\beta m \lambda_{\mathsf{max}}(\boldsymbol{\Omega}_1' \boldsymbol{\Omega}_1) \mathbf{I}_{N_p} & \mathbf{0} \\ \mathbf{0} & 2\beta m \lambda_{\mathsf{max}}(\boldsymbol{\Omega}_2' \boldsymbol{\Omega}_2) \mathbf{I}_{N_p} \end{pmatrix}.$$

- Pixel-wise update involves one 2×2 matrix per voxel:

$$\mathbf{x}_j^{(i+1)} = \arg\min_{\mathbf{x}_j} \frac{1}{2}\|\mathbf{y}_j - \mathbf{A}_0\mathbf{x}_j\|_{\mathbf{W}_j}^2 + \frac{1}{2}\|\mathbf{x}_j - \boldsymbol{\xi}_j^{(i)}\|_{\mathbf{M}_j}^2, \qquad (6)$$

  where $\mathbf{M}_j \in \mathbb{R}^{2\times 2}$ is a diagonal weighting matrix for $(x_{1j}, x_{2j})^T$.
- Quadratic majorizer used within FGM (Fast Gradient Method)[8] (Instead of usual generic Lipschitz constant)

$$\text{blockdiag}\{\mathbf{A}_0'\mathbf{W}_j\mathbf{A}_0 + \mathbf{M}_j\}^{-1} \quad \text{vs} \quad \frac{1}{L}$$

[8] [Nesterov, Doklady AN USSR, 1983]

Outline

- **Training**
  - Training set: patches extracted from five slices of water and bone images of XCAT phantom, respectively.
  - Patch size 8×8 and patch stride 1×1.

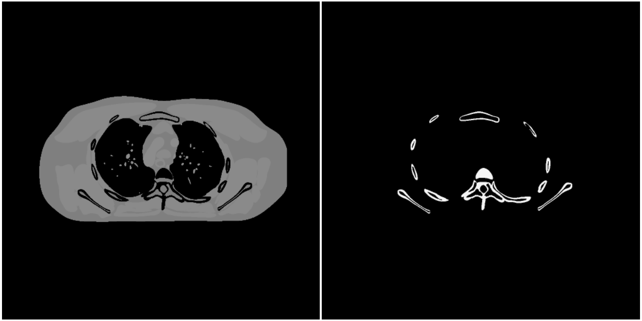

Example training image slices for water (left) and bone (right).

[9] [Segars et al., MP, 2008]

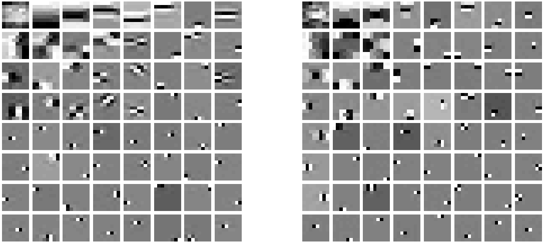

Learned transforms $\boldsymbol{\Omega}_l$ for water (left) and bone (right).

- Transforms $(\boldsymbol{\Omega}_1, \boldsymbol{\Omega}_2)$ are initialized with 2D DCT.
- Rows of learned transforms shown as 8×8 patches.

DECT Simulation Setup

- NCAT phantom sinogram simulation:
  - Image size: 1024×1024
  - Poly-energetic source: 80kVp and 140kVp with 1.86×10^5 and 1×10^6 incident photons per ray
  - Sinogram size: 888×984
  - Reconstruct attenuation images via FBP
- Reconstruction and decomposition:
  - Image size: 512×512
  - Pixel size: 0.98×0.98 mm^2
  - Optimal parameter combinations to achieve the best image quality and decompositon accuracy

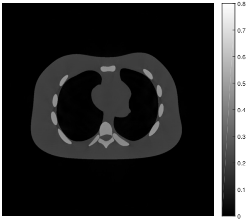

High energy atten. image

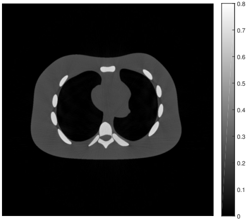

Low energy atten. image

RMSE Comparison

Table: RMSE of estimated material densities in mg/cm^3.

Method	Direct Inversion	DECT-EP	DECT-ST
Water	77.7	39.5	**35.1**
Bone	78.7	53.8	**46.2**

- Direct Inversion: obtain material images directly by matrix inversion
- DECT-EP: Hyperbola Edge-Preserving regularizer with $\delta_1 = 0.01\,\mathrm{g/cm^3}$ and $\delta_2 = 0.02\,\mathrm{g/cm^3}$
- DECT-ST further decreases RMSE achieved by DECT-EP

Results

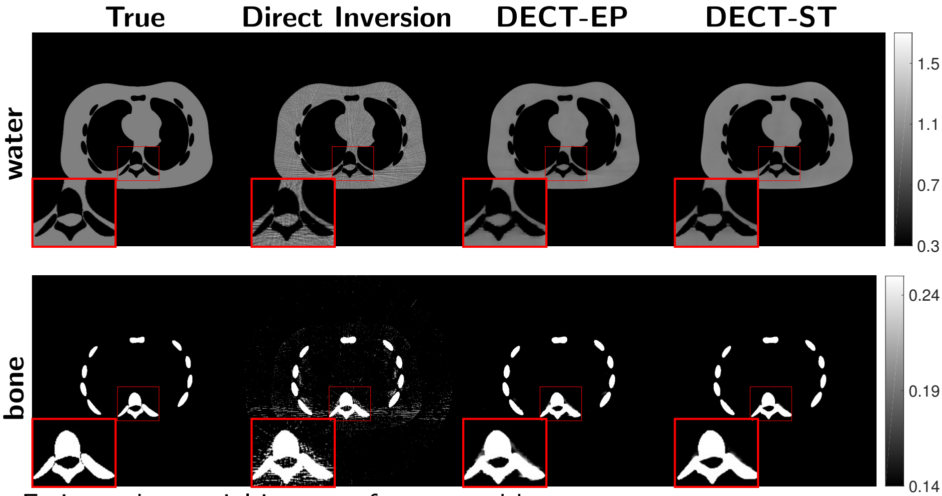

Estimated material images of water and bone,
display window [0.3 1.7] g/cm^3 and [0.14 0.25] g/cm^3, respectively.

Patient Study

- Obtained by Siemens SOMATOM Force CT scanner using DECT imaging protocols
- Dual-source at 150 kVp and 80kVp

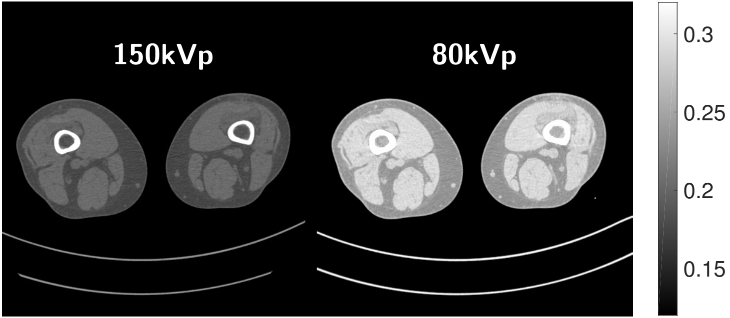

Thigh CT images of a patient. Display window is [0.12 0.32] cm^{-1}.

Results

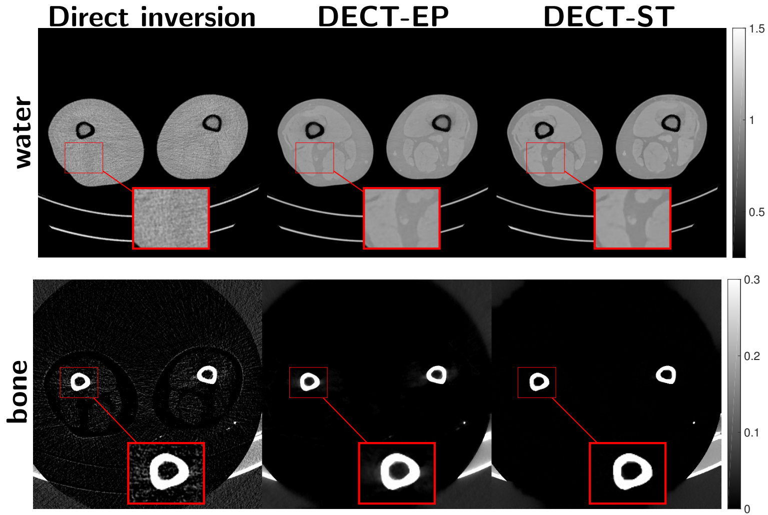

Estimated material images of water and bone;
display window [0.25 1.5] g/cm^3 and [0 0.3] g/cm^3, respectively.

Outline

- **Conclusions**
  - We proposed DECT-ST that combines an image-domain WLS term with regularizer involving learned sparsifying transforms.
  - DECT-ST outperformed the DECT-EP method (which uses a fixed finite differencing type sparsifying model) in terms of image quality and material decomposition accuracy.
- **Future Work**
  - Investigate cross-material ST that accounts for correlation between material images.
  - Investigate decomposition methods using a more accurate DECT measurement model[10] with ST-based regularization.

[10] [Long & Fessler, IEEE T-MI, 2014]

Thanks for your attention!